Available online at www.sciencedirect.com

jmr&t Journal of Materials Research and Technology

journal homepage: www.elsevier.com/locate/jmrt

Original Article

Specific energy modeling of abrasive cut off operation based on sliding, plowing, and cutting

Muhammad Rizwan Awan [a,*], *Hernán A. González Rojas* [a], *José I. Perat Benavides* [b], *Saqib Hameed* [a], *Abrar Hussain* [c], *Antonio J. Sánchez Egea* [a]

[a] *Department of Mechanical Engineering, Universitat Politechnica De Catalunya(UPC) Barcelona-Tech, The Superior University Lahore, Spain*

[b] *Department of Electrical Engineering, Universitat Politechnica De Catalunya(UPC) Barcelona-Tech, Spain*

[c] *Department of Mechanical and Industrial Engineering, Tallinn University of Technology, Estonia*

ARTICLE INFO

Article history:
Received 7 February 2022
Accepted 30 March 2022
Available online 13 April 2022

Keywords:
Specific energy model
Abrasive cutting
Sliding energy
Plowing energy
Inconel-718
Cutt-off grinding

ABSTRACT

Studying the specific energy during material removal mechanism at micro-scale provides a better understanding of energy transition between different material removal regimes. Modeling of specific energy into components of sliding, plowing and cutting helps to analyze the influence of grain properties process parameters, and mechanical properties on energy transition between different phases of material removal. Present research put forth the comprehensive model of specific energy consumption for abrasive cut off operating based on the individual models of primary and secondary rubbing energies, specific plowing energy and specific cutting energy. Materials of SS201, Inconel 718, Al 1100, Al 7075 and oxygen free copper (OFC– C10100) have been employed while cutting with semi super abrasive cubitron cut off wheel. Model validation on experimental data revealed that triangular shape of cubitron grits significantly influenced the plowing energy and played an important role in energy transition between different material removal regimes. Moreover, cutting conditions and material properties also affected the overall specific energy consumption, dominance of particular specific energy components and machinability of the materials.

1. Introduction

Grinding being a multi-point cutting operation consumes high specific energy in comparison to machining, due to rubbing, and plowing of irregular shaped abrasive grits [1]. Studying the material removal mechanism of grinding helps to better understand the mechanics of the grinding process [2]. The material removal mechanism in grinding on microscale was first analyzed by Hahn, who proposed the three material removal regimes as rubbing, plowing, and cutting [3]. Rubbing or sliding is the first stage of grain interaction with the work piece; elastic deformation takes place in this phase with a negligible amount of material removal [4]. After sliding,

* Corresponding author.
E-mail address: mrawan@kth.se (M.R. Awan).

https://doi.org/10.1016/j.jmrt.2022.03.185

further increase of force, grain penetration into the work piece is increased leading to plowing phase, both elastic and plastic deformation takes place in this phase [5]. With further increase of shearing stress, tearing of the material in the form of chips takes place, known as the cutting phase [6].

Recent studies on abrasive grit work piece interaction divide the sliding energy into primary and secondary rubbing energies. Manoj et al. [7] and Singh et al. [8] conducted abrasive grit tests to analyze the sliding and plowing energies. They demonstrated two kinds of rubbing energies during grain contact with the work piece, primary and secondary rubbing energies. Primary rubbing energy is due to the grit sliding over the work piece without penetration, which is caused by the bluntness of the abrasive grit, and this energy dissipation does not participate in the material removal process. While secondary rubbing energy is caused by the rubbing action between abrasive grits and work piece along the cutting edge over the whole cutting path [9]. The highly negative angle of abrasive grit is mostly responsible for secondary rubbing energy [10]. The highly negative rake angle of abrasive grits displaces material, leading to the plowing phase [11,12]. Plowing energy is influenced by the grit shape, size, orientation, and other parameters like depth of cut feed rate, and wheel speed [8]. Vathaire et al. [13] employed an upper bound model to study the surface plowing phenomenon by using a pyramidal indentor. Ghosh et al. [14] and Singh et al. [15] suggested that effective negative rake angles on the leading face of grain significantly increase the plowing energy in single grit grinding and indentation tests. In another study, Singh et al. [9] formulated a specific plowing energy model in terms of scratch hardness and the ratio of pile-up height to the grit penetration depth, both of them are the functions of grinding process parameters. Moreover, specific plowing energy was more prominent at the low depth of cut for composite ceramics. The pile-up ratio is another measure to understand material displacement during the plowing phase [16]. Manoj et al. [17] analyzed the specific plowing energy in single grit tests and determined that a higher pileup ratio at lower feed rates presents a more plowing phenomenon, which is the reason for the size effect. So, high sliding and plowing energy at lower feed rates are the reason for the higher specific energy of grinding. Matsu et al. [18] used CBN and diamond grits for single grit scratch tests to measure pile-up material under different testing conditions. With the increase of grain depth, effective negative rake angle reduces, which reduces the plowing energy. So, high sliding and plowing energy at lower feed rates are the reason for the higher specific energy of grinding [2]. As the grit further penetrates, the plowed material is not able to withstand shearing stress, and the material is removed in the form of chips, leading to the cutting phase [19]. Malkin opined that specific chip formation energy is the minimum energy required to produce chips, has a constant value, and is equal to the adiabatic melting energy of the work piece, however melting does not occur in grinding [20,21].

Owing to the large specific energies in grinding, more energy-efficient grinding processes with large material removal rates have been developed. HEDG offers high material removal rate at low specific energy [22]. In HEDG, stock removal is achieved at a high down feed rate (0.25–5 mm/s) combined with high grinding velocities [23]. The modeling of specific energy consumption for HEDG has been extensively discussed [24,25]. Ghosh et al. [14] Identified main energy consumers in high efficiency deep grinding as primary rubbing energy, secondary rubbing energy, specific plowing energy, and specific cutting energy. Similar to HEDGE, in terms of high down feed rates and cutting velocities, abrasive cut off operation is another bulk material removal process [26].

In comparison to detailed studies on specific energy characterization, modeling, and analysis of surface grinding [8,27–31], a few attempts have been made to evaluate and characterize specific energy of abrasive cut off operation into sliding, plowing, and cutting [32]. However, the comprehensive models of sliding, plowing, and specific cutting energy, their relationship, and sensitivity with process parameters for abrasive cut off operation have not been evaluated yet. The present study is an attempt to bring forward comprehensive models of specific energy components of metal cutting with thin cubitron discs. In model development, grit shape has been taken into consideration which answered the sensitivity of specific energy components in relation to material removal rate. Superalloy, ferrous and non ferrous metals have been studied in this research. The experiments have been conducted using cubitron wheels due to high hardness, thermal resistance, efficient and fast cutting ability [5,33,34].

2. Models of specific energy

The model is developed based on specific energy consumption (SEC) of a thin cut off wheel. This model incorporates the sliding, plowing, and cutting mechanisms and obtains an expression of the SEC associated with each of these mechanisms. The model is understood as the superposition of the mechanical power consumed by each of the aforementioned mechanisms. The constants of the model are obtained by a least-squares regression of the experimentally measured SEC. The model is the result of experimental constants and expressions that respond to the physics of the three mechanisms associated with disc cutting. The specific energy consumed is the mechanical power required to remove a unit volume of material, and is defined as the ratio between mechanical power consumed and material removal rate [2].

$$SEC = \frac{P_m}{Q_w} \tag{1}$$

In turn, the material removal rate is defined as the product of the cut-off wheel feed rate V_f multiplied by the cutting section perpendicular to the feed rate vector. The cross-section is defined by the product of the cutting thickness of the cut-off wheel e_d and the thickness of the cutting material e_m as shown in Fig. 2.

$$Q_w = V_f e_d e_m \tag{2}$$

2.1. *Plowing energy model*

The assumption that the entire volume traversed by the abrasive grain is removed by the abrasive wear mechanism is not correct [35]. In ductile metals, part of the material

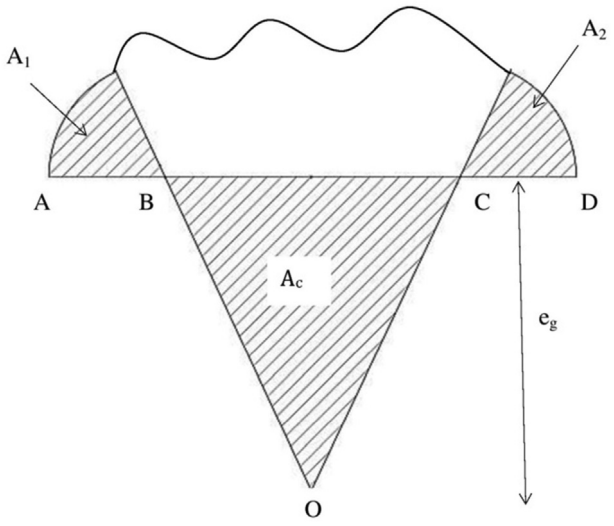

Fig. 1 – Abrasion and build up on ductile material.

accumulates at the edges of the groove defined by the abrasive, as shown in Fig. 1

The f_{ab} factor is introduced to define the ratio between the volume of material removed from the surface and the volume of the groove formed by the movement of the abrasive.

$$f_{ab} = 1 - \frac{(A_1 + A_2)}{A} \tag{3}$$

where $(A_1 + A_2)$ is the cross-sectional area of material accumulated around the edges of the groove, A is the cross-sectional area of material defined by the movement of the abrasive, f_{ab} is a dimensionless parameter defined in the range (0–1) [36]. If f_{ab} is equal to zero, all the material in the groove formed by the movement of the abrasive grain is stacked. In this case, there is no chip formation. If f_{ab} is equal to 1, all the material in the groove formed by the movement of the abrasive grain is removed from the work piece, which would be the case of an ideal cutting. The rate of material removed per grit Q_g is defined as

$$Q_g = f_{ab} \times A_c \times V_c \tag{4}$$

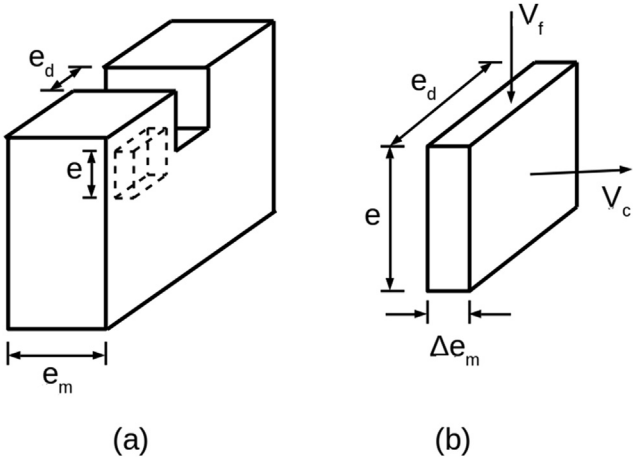

Fig. 2 – Macroscopic material removal rate.

where V_c is the cutting speed defined by the peripheral speed of the disc. A is a function of the square of the depth of cut e_g of a pyramidal grit multiplied by a constant C_1 which depends on the angle defining the pyramid. The rate of material removed by all the grits is a function of the grit number N and the equivalent depth of cut e, among other parameters and constants [5]. The rate of material removed by a cut-off wheel during the plowing can be defined as.

$$Q_{pl} = N \cdot f_{ab} \cdot e^2 C_1 \cdot V_c \tag{5}$$

At the macroscopic level, the volume of material removed can be estimated from a differential volume associated with the cavity generated per disc as shown in Fig(2). In Fig. 2a, the rate of material removed can be defined from Eq. (2) or as the product of the shear velocity V_c by the section perpendicular to the vector V_c as shown in Fig. 2b. This ratio of volume removed allows estimation of the equivalent depth of cut e.

$$e = \frac{V_f}{V_c} e_m \tag{6}$$

The Specific Energy Consumed with plowing is defined as

$$SEC_{pl} = \frac{C_{pl}}{e^2 \cdot V_c} \tag{7}$$

where C_{pl} is a constant function of the number of active grit, the shape of the grit, f_{ab} factor, and the power of plowing P_{pl}. Replacing (6) in (7) and assuming that the rate of material removal as defined in Eq. (2)

$$SEC_{pl} = \frac{C_{pl} V_c e_d^2}{Q_w^2} \tag{8}$$

2.2. *Primary rubbing energy*

The primary rubbing energy is the phenomena of rubbing of grit tip against the work piece surface without penetration [36]. Vijayender defined the primary friction energy as the energy dissipated by the grit contact with the material surface without penetration [8]. The grit shape has an edge radius that rubs against the material surface due to the structural rigidity of the machine, producing a primary frictional force.

The Specific Energy Consumed with primary rubbing is defined as

$$SEC_{pr} = \frac{C_{pr} V_c}{Q_w} \tag{9}$$

where C_{pr} is the coefficient of primary rubbing energy. This constant is a function of the friction force, the number of active cutting grits, and the power of primary rubbing P_{pr}.

2.3. *Secondary rubbing energy*

Secondary rubbing occurs between the cutting edge and the work piece mainly due to high (negative) grit angles of the abrasive grits [8]. Secondary friction occurs mainly along the entire length of the scratch, produced by the abrasive grit along with the area BOC as shown in Fig. 2. As the plowed material is not so stiff, the friction between the surfaces AB and CD is assumed to be negligible. Specific Energy Consumed with secondary rubbing is defined as

$$SEC_{sr} = \frac{C_{sr} \cdot V_c}{Q_w} \tag{10}$$

where C_{sr} is a constant resulting from the product of the average value of the tangential shear force for a grain by the number of active grit rubbing against the surface of the material.

2.4. Specific cutting energy

The chip formation timescale as stated above indirectly supports the Malkin hypothesis [2]. Malkin's hypothesis defines the specific shear energy as a material property, where the SCE does not depend on the cutting conditions of the process and therefore both can be assumed as a constant in this model. The time scale hypothesis suggests that the chip formation phenomenon is very fast, so that the entire SCE is associated with the sublimation energy of the material and therefore depends mainly on the material. The behavior of SCE as a function of shear conditions could be a future work direction.

$$SCE = \frac{P_c}{Q_w} \tag{11}$$

where P_c is the power of chip formation.

2.5. Energy conservation in cutting through the abrasive disc

Applying the principle of energy conservation, the energy consumed per unit time during the metal cutting with abrasive discs is the sum of the energies consumed by each of the above-mentioned mechanisms, sliding, plowing, and chip formation.

$$SEC = SEC_{pl} + SEC_{pr} + SEC_{sr} + SCE \tag{12}$$

Replacing (8), (9), (10), and (11) in (12) gives the energy conservation model for cutting with abrasive discs.

$$\frac{P_M}{Q_w} = \frac{C_p V_c e_d^2}{Q_w^2} + \frac{C_{sl} V_c}{Q_w} + SCE \tag{13}$$

where. $C_{sl} = C_{pr} + C_{sr}$

The model constants, right-hand side of Eq. (13) shown in Table 1, are obtained by performing a least-squares regression of metal cutting experiments through thin abrasive discs.

3. Experimental validation

The specific energy consumption is the defined as the quotient of cutting power and material removal rate as defined in Eq. (2). To measure both of these parameters, experiments with the thin cutting disc were performed by adopting the same methodology as presented by Awan et al. [32]. The methodology makes use of two different experimental settings to measure the mechanical cutting power as shown in Fig. 3.

Table 1 – Coefficients of Model and materials hardness.

Material	C_{pl}	C_{sl}	SCE	R^2	Hardness (Brinell)
Al 7075	7.5E-18	0.0011	17.38	0.970	150
Al 1100	7.5E-03	0.0016	18.59	0.952	32
OFC-C10100	6.4E-18	0.0076	8.67	0.969	95
Inconel-718	3.4E-19	0.0025	22.92	0.998	340
SS201	1.5E-03	0.0009	20.82	0.957	121

First, the standard angle grinder is coupled with a dynamometer, which measures different characteristics like torque, mechanical cutting power (P_m), affective electric power (E_e), and rotational speed (r/min) under different loading conditions. Affective electric power is capable of transforming electrical energy in to work and is the product of instantaneous current, voltage and power factor. It is actual power consumed by the load and is expressed in watts. The relationship between mechanical cutting power (P_m) and affective electric power (E_e) has been used to calculate the regression equation for the estimation of mechanical cutting power (P_m), during experiments with a thin cutting disc. The experiments with thin cutting discs have been performed using a smart automated machine as shown in Fig. 3b. This machine is self-developed and automated through microcontroller Arduino Uno. Cubitron cutting disc of 1 mm, with précised triangular pyramid-shaped grains, precisely cuts the materials at different feed rates. The downward movement of the machine in response to the feed rate selection is controlled by a stepper motor, which is programmed through Arduino Uno. Four predefined feed rate values of 0.54 mm/s, 0.61 mm/s, 0.9 mm/s and 1.488 mm/s have been chosen for this experiment. The setup provides the option to change the feed rate range by changing the no of steps in the motor driver TB6600. The limit switches, programmed through Arduino Uno, actuate to keep the machine within the permissible work limits. The power analyzer measures the electrical power (E_e) consumed during metal cutting, which is then stored in a computer through a channel recorder. This electrical power (E_e) consumed during metal cutting is then used to find the corresponding values of mechanical cutting power through the regression equation obtained earlier in the first step.

The material removal rate defined in Eq. (2) is a product of feed rate V_f, and perpendicular cutting area. The feed rate V_f is a function of the stepper motor, and is evaluated by the study of generalized coordinates [37], and is experimentally verified by the time taken for the cutting disc to cuts through the material.

3.1. Materials and cutting tool

Materials employed for experimentation in this study are Inconel-718, Al 7075, Al 1100, oxygen free copper (OFC−C10100), and SS201. Super abrasive cubitron cutting disc has been used to cut materials. It is made up of resin bonded precision shaped abrasive material with glass fibre reinforcement. The thickness of cutting disc is 1 mm, with diameter of 115 mm and maximum cutting speed of 80 m/s. The Cubitron cut off wheel is preferred due to precisely shaped triangular grits, which enable fast cutting and are highly suited for hard materials like Inconel-718 [38]. The experimental data has been collected and processed by the same tools used in the previous study [32]. The experimental data of cutting power (P_m), and material removal rate (Q_w) in Eq. (2) has been adjusted using the least square regression method

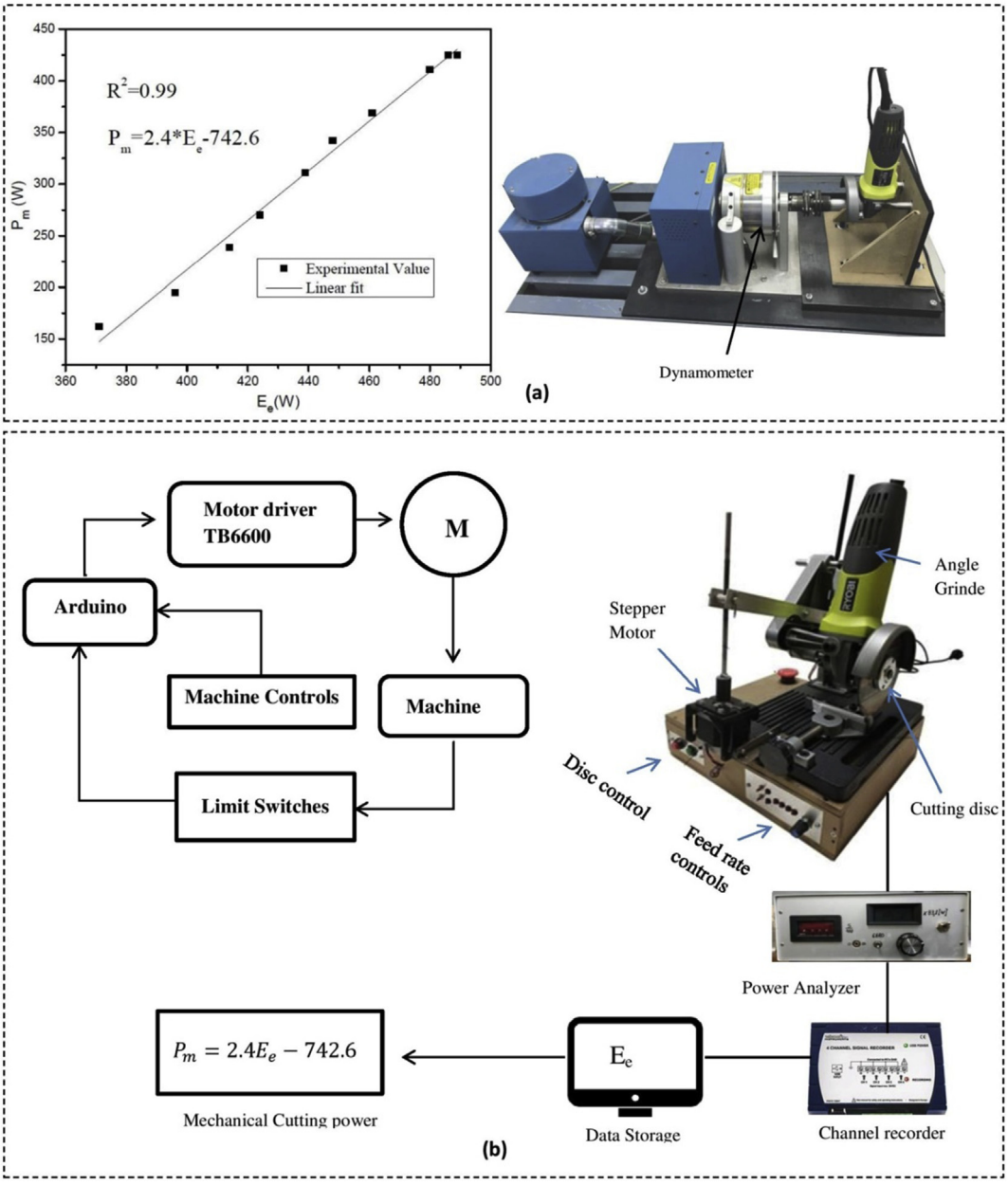

Fig. 3 – Experimental set up for metal cutting with thin discs.

with multiple iterations to find the model coefficients in Eq. (13). The values of model coefficients along with correlation error and hardness values of materials are given in Table 1. The correlation error square close to unity suggests a good fit of the developed model with the experimental results.

4. Results and discussion

The good correlation between the developed model and experimental data reinforces the idea that SCE has an asymptotic behavior with the rate of material removed. As shown in Fig. 4, with an increase in material removal rate, specific energy consumption decreases, a trend that is similar to previous research in grinding [8,25,27,39]. The concept of ductility helps to understand the overall energy consumption for materials. In ductile materials, the gumminess of work piece materials due to heat generation, and higher fracture toughness in comparison to brittle materials increases the machining difficulty, and consequently, more specific energy is required during metal cutting [40]. For this reason, the specific energy consumption of ductile materials like OFC-C10100 and Al-1100 is higher in comparison to other materials at the same material removal rate. In the grinding of hard and less ductile materials, the crack growth rate during cutting with abrasive grits is higher, which reduces the energy required to deform the material [41]. For this reason, hard and less ductile materials of SS201 and Al 7075, are comparatively consuming less specific energy. Among the materials, Inconel-718 is consuming higher specific energy. This is due to

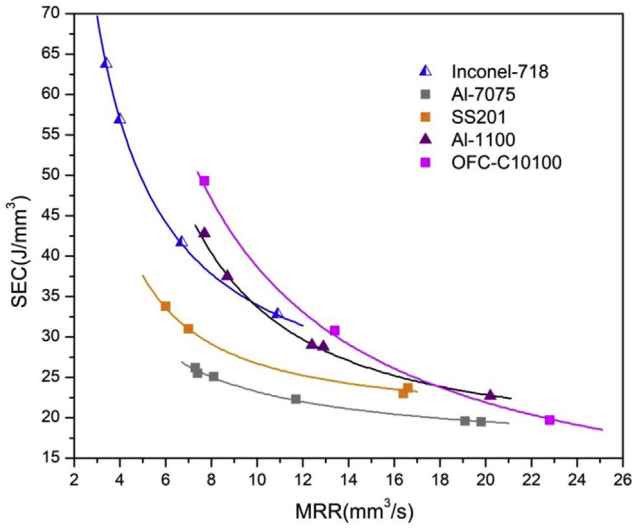

Fig. 4 – SEC relationship with material removal rate for materials.

its high value of hardness, higher strength, and higher resistance to cutting [42].

High stability at elevated temperature, presence of hard carbides in the microstructure and work hardening during machining are contributing factors for poor machinability and specific cutting energy of Inconel-718 [42,43]. An increase in hardness, increases the resistance to penetration of the abrasive grain, so grinding energy increases [44]. However, in comparison to the difference in hardness of Inconel-718 with other hard materials, the difference in specific energy consumption is not that much higher. This is due to the high suitability of cubitron wheels for grinding of Inconel-718, which reduces the abrasive resistance of the material, and can remain inert to higher cutting temperatures due to the higher strength of the Inconel-718 [42,45,46]. For Al-7075, the specific energy consumption is lowest and the trend line is almost close to straight, which is an indication of major dominance of SCE at low and high material removal rates. Abachi et al. [47] attributed the low resistance to fracture due to fast crack initiation and crack propagation within the microstructure.

The comparison of SCE of the materials shown in Table 1 indicates that SCE of hard and tough materials like Inconel-718, and SS 201 are higher among specimens. The OFC-C10100 has the lowest SCE among specimens although its SEC values are higher among most of the materials. This is due to the ductile-brittle failure mode in OFC-C10100 [48], which reduces the SCE.

Fig. 5 shows the change in the contribution of specific energy components with an increase in material removal rate. It also reveals the influence of using cubitron on specific energy components. It is quite evident that SCE is the most dominant form of energy dissipation for most cases. It can be seen in Fig. 5b that there is no plowing in materials of Al 7075, Inconel 718, and OFC-C10100 for the range of material removal used in this experiment. The dominance of SCE and absence of plowing energy in some materials is attributed, to the efficient cubitron grits. Cubitron is semi-super abrasives, with

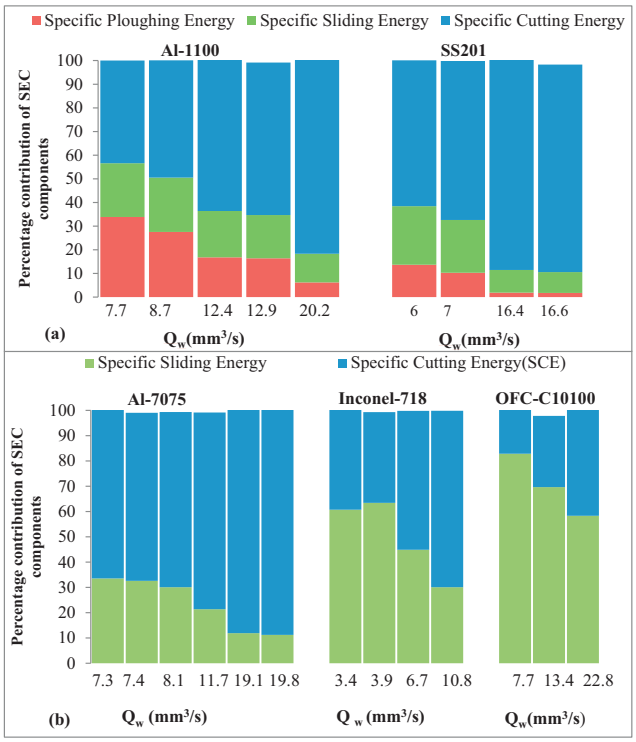

Fig. 5 – Contribution of Sliding, plowing, and SCE in material removal for materials of. (a) Al-1100, SS201 (b) Al-7075, Inconel-718 and OFC-C10100.

precision-shaped triangular grains which enable fast cutting [49].

According to Malkin [2], it is the possibility that plowing energy might not appear during grinding with super abrasives. He attributed the possibility of the absence of plowing energy to the precision pyramidal shape of abrasive grains. The cutting points are much sharper and pointed, and at the faster cutting speeds, the transition from plowing to cutting phase is fast, which reduces the plowing force. Owing to the fast and précised cutting ability of abrasive grain, SCE is the most dominant form of energy consumption in most of the material.

Moreover, model Eq. (13) also indicates that specific plowing energy is more sensitive to material removal rate in comparison to sliding energy. It is changing inversely with the square of material removal rate. It means a small change in material removal can bring a significant change in specific plowing energy. At a very low material removal rate, the appearance of the plowing phenomenon could be possible. So, it might be possible that for these materials, there is a plowing phenomenon below the defined range of material removal rate used in this experiment.

During grinding, material properties played an important role in defining the dominance, presence, and insignificance of specific energy components. For instance, Al 1100, and OFC-C10100, being both ductile materials have shown different behavior in this experiment. The energy consumption in copper is dominated by the sliding phenomenon. The apparent reason could be the high elasticity of Cu, in comparison to Al 1100 [50,51]. As the sliding phenomenon takes

place in the elastic regime of material deformation, so high value of elasticity indicates more resistance to rubbing and increases the sliding energy. The absence of plowing phenomenon in OFC-C10100 is due to the grain refinement and dynamic recrystallization generation during the cutting process, which caused the fracture transformation from ductile to brittle [48]. So, after the elastic deformation, as the material entered into the plastic state, the transformation to brittle nature, along with cutting action of sharper and pointed abrasive grits might have made the crack growth so fast that eliminated the plowing energy and also reduced the SCE. The lower SCE in the brittle state is well in agreement with the previous research on abrasive cut off operation [39].

On the other hand, Al 1100 has low hardness, and failure is characterized by large strain deformation [52,53]. For this reason, even with pointed and sharp cutting grains, the transition from elastic to plastic deformation takes time, and plowing is significant at low material removal rates. The high SCE of Al 1100 is attributed to an increase in temperature in the plastic deformation zone, which reduced the hardness and increased the ductility of the material, so the energy required to produce chips increased [54].

Although SS201 is a hard material, but some plowing still appears at a low material removal rate. The appearance of plowing is attributed to the very low material removal rate in SS201. The metal bar thickness of SS 201 is 5 mm in comparison to other materials which ranged from 9 to 11 mm. As a result, the material removal rate is comparatively low. As formulated in model Eq. (13), plowing is very sensitive to material removal rate, so at a small material removal rate, plowing energy appeared in SS 201 as shown in Fig. 5b. The careful observation also reveals that small increases in material removal rate, the decreases or disappearance of plowing energy is also fast, in comparison to sliding energy. This proves the validation of model Eq. (13)

The absence of plowing in Inconel-718 is not in agreement with the previous research on grinding. Plowing appears to be a significant phenomenon in experimentation conducted by Sinha et al. [17] during surface grinding of Inconel-718. Similarly Tahsin et al.'s [55] study during single grit grinding of Inconel-718, also revealed the prominent plowing phenomenon. However, in these studies, the depth of cut and in feed rates are low, which is the reason for the prominent plowing energy phenomenon. The high SCE and SEC values in Inconel-718 could also be due to the work hardening of the material during the grinding process [56].

5. Conclusion

In this study, the detailed models of primary and secondary rubbing energies, specific plowing energy, and specific cutting energy are developed and validated through experimental data. The developed model enabled us to understand the contribution of sliding, plowing, and SCE with change in material removal rate during abrasive cut off operation. It was found out that grit shape has a notable effect on material removal mechanism and the corresponding specific energy consumption. The model development and validation revealed that due to sharp, and pointed triangular abrasive grits, plowing energy turned out to be more sensitive to material removal rate than sliding. It changes inversely with the square of material removal rate, due to the sharpness of cubitron grits. For the material removal range used in this experiment, plowing energy did not appear for the materials of Cu, Al 7075, and Inconel 718. The brittle fracture in these materials, combined with the fast cutting of sharp triangular grits made the transition from sliding to specific cutting energy very fast that plowing energy could not appear. In SS 201, plowing appeared due to the low material removal rate resulting from the small thickness of the material used. Due to the high efficiency of cubitron grits, SCE remained the most dominant specific energy component in most of the materials. Cutting with cubitron discs minimized the redundant energies of sliding and plowing.

Declaration of Competing Interest

The authors declare that they have no known competing financial interests or personal relationships that could have appeared to influence the work reported in this paper.

REFERENCES

[1] Principles of abrasive processing - Milton C. Shaw - Oxford University Press. https://global.oup.com/academic/product/principles-of-abrasive-processing-9780198590217?cc=us&lang=en&. Accessed 25 Mar 2021.

[2] Malkin S, CG. Grinding technology: theory and applications of machining with abrasives. New York: Industrial Press; 2008.

[3] R.S. Hahn, On the nature of the grinding process..., - Google Scholar. https://scholar.google.com/scholar?hl=en&as_sdt=0%2C5&q=R.S.+Hahn%2C+On+the+nature+of+the+grinding+process%2C+in%3A+Proceedings+of+the+3rd+International+Machine+Tool+Design+%26+Research+Conference%2C+Manchester%2C+1962%2C+pp.+129–154&btnG=. Accessed 26 Mar 2021.

[4] Öpöz TT, Chen X. Experimental investigation of material removal mechanism in single grit grinding. Int J Mach Tool Manufact 2012;63:32–40. https://doi.org/10.1016/j.ijmachtools.2012.07.010.

[5] Rowe WB. Principles of modern grinding technology. 2013.

[6] Stachowiak GW, Batchelor Andrew WGB. Experimental methods in tribology: Introduction. Elsevier 2004.

[7] Sinha MK, Ghosh S, Paruchuri VR. Modelling of specific grinding energy for Inconel 718 superalloy. Proc Inst Mech Eng Part B J Eng Manuf 2019;233:443–60. https://doi.org/10.1177/0954405417741513.

[8] Singh V, Venkateswara Rao P, Ghosh S. Development of specific grinding energy model. Int J Mach Tool Manufact 2012;60:1–13. https://doi.org/10.1016/j.ijmachtools.2011.11.003.

[9] Singh V, Ghosh S, Rao PV. Comparative study of specific plowing energy for mild steel and composite ceramics using single grit scratch tests. Mater Manuf Process 2011;26:272–81. https://doi.org/10.1080/10426914.2010.526979.

[10] (4) (PDF) An improved model for specific energy estimation in surface grinding of Inconel 718. https://www.researchgate.net/publication/286932438_An_Improved_Model_for_Specific_Energy_Estimation_in_Surface_Grinding_of_Inconel_718. Accessed 11 Apr 2021.

[11] Paul S, Chattopadhyay AB. A study of effects of cryo-cooling in grinding. Int J Mach Tool Manufact 1995;35:109–17. https://doi.org/10.1016/0890-6955(95)80010-7.
[12] Paul S, Chattopadhyay AB. Effects of cryogenic cooling by liquid nitrogen jet on forces, temperature and surface residual stresses in grinding steels. Cryogenics 1995;35:515–23. https://doi.org/10.1016/0011-2275(95)98219-Q.
[13] De Vathaire M, Delamare F, Felder E. An upper bound model of ploughing by a pyramidal indenter. Wear 1981;66:55–64. https://doi.org/10.1016/0043-1648(81)90032-6.
[14] Ghosh S, Chattopadhyay AB, Paul S. Modelling of specific energy requirement during high-efficiency deep grinding. Int J Mach Tool Manufact 2008;48:1242–53. https://doi.org/10.1016/j.ijmachtools.2008.03.008.
[15] Singh V, Patnaik Durgumahanti US, Venkateswara Rao P, Ghosh S. Specific ploughing energy model using single grit scratch test. Int J Abras Technol 2011;4:156–73. https://doi.org/10.1504/IJAT.2011.041609.
[16] Öpöz TT, Chen X. Experimental investigation of material removal mechanism in single grit grinding. Int J Mach Tool Manufact 2012;63:32–40. https://doi.org/10.1016/J.IJMACHTOOLS.2012.07.010.
[17] Sinha MK, Ghosh S, Paruchuri VR. Modelling of specific grinding energy for Inconel 718 superalloy. Proc Inst Mech Eng Part B J Eng Manuf 2019;233:443–60. https://doi.org/10.1177/0954405417741513.
[18] Matsuo T, Toyoura S, Oshima E, Ohbuchi Y. Effect of grain shape on cutting force in superabrasive single-grit tests. CIRP Ann - Manuf Technol 1989;38:323–6. https://doi.org/10.1016/S0007-8506(07)62714-0.
[19] Chen X, Öpöz TT. Characteristics of material removal processes in single and multiple cutting edge grit scratches. Int J Abras Technol 2014;6:226–42. https://doi.org/10.1504/IJAT.2014.060693.
[20] Malkin S, Joseph N. Minimum energy in abrasive processes. Wear 1975;32:15–23. https://doi.org/10.1016/0043-1648(75)90201-X.
[21] Malkin S. Grinding processes. In: Encyclopedia of tribology. Springer US; 2013. p. 1573–80.
[22] Klocke F, Brinksmeier E, Evans CJ, Howes T, Inasaki I, Minke E, et al, Stuff D high-speed grinding - fundamentals and state of the art in Europe, Japan, and the USA. vol. 46.
[23] T. Tawakoli, High efficiency deep grinding, VDI-Verlag - Google Scholar. https://scholar.google.com/scholar?hl=en&as_sdt=0%2C5&q=T.+Tawakoli%2C+High+Efficiency+Deep+Grinding%2C+VDI-Verlag+and+Mechanical+Engineering+Publications+Ltd.+%28MEP%29%2C+London%2C+1993.&btnG=. Accessed 5 Jul 2021.
[24] Jin T, Stephenson DJ. Analysis of grinding chip temperature and energy partitioning in high-efficiency deep grinding. Proc Inst Mech Eng Part B J Eng Manuf 2006;220:615–25. https://doi.org/10.1243/09544054JEM389.
[25] Batako ADL, Morgan MN, Rowe BW. High efficiency deep grinding with very high removal rates. Int J Adv Manuf Technol 2012;66(9):1367–77. https://doi.org/10.1007/S00170-012-4414-7.
[26] Bing Hou Z, Komanduri R. On the mechanics of the grinding process-Part I. Stochastic nature of the grinding process. Int J Mach Tool Manufact 2003;43:1579–93. https://doi.org/10.1016/S0890-6955(03)00186-X.
[27] Nápoles Alberro A, González Rojas H, Sánchez Egea A, Hameed S, Peña Aguilar R. Model based on an effective material-removal rate to evaluate specific energy consumption in grinding. Materials 2019;12:939. https://doi.org/10.3390/ma12060939.
[28] Kannappan S, Malkin S. Effects of grain size and operating parameters on the mechanics of grinding. J Manuf Sci Eng Trans ASME 1972;94:833–42. https://doi.org/10.1115/1.3428258.
[29] Ghosh S, Chattopadhyay AB, Paul S. Study of grinding mechanics by single grit grinding test. Int J Precis Technol 2010;1:356. https://doi.org/10.1504/ijptech.2010.031663.
[30] Sinha MK, Paruchuri VR, Kumar P, Ghosh S, Venkateswara Rao P (2015) An improved model for specific energy estimation in surface grinding of Inconel 718 functional surfaces view project sustainable manufacturing view project an improved model for specific energy estimation in surface grinding of Inconel 718.
[31] Sinha MK, Ghosh S, Paruchuri VR. Modelling of specific grinding energy for Inconel 718 superalloy. Proc Inst Mech Eng Part B J Eng Manuf 2019;233:443–60. https://doi.org/10.1177/0954405417741513.
[32] Awan MR, Rojas HAG, Benavides JIP, Hameed S. Experimental technique to analyze the influence of cutting conditions on specific energy consumption during abrasive metal cutting with thin discs. Adv Manuf 2021:20211–202112. https://doi.org/10.1007/S40436-021-00361-2.
[33] Marinescu ID, Rowe WB, Dimitrov B, Inasaki I. Abrasives and abrasive tools. In: Tribology of abrasive machining processes. Elsevier; 2004. p. 369–455.
[34] Rowe WB. Grinding wheel developments. In: Principles of modern grinding technology. Elsevier; 2009. p. 35–58.
[35] Fang L, Xing J, Liu W, Xue Q, Wu G, Zhang X. Computer simulation of two-body abrasion processes. Wear 2001;250:1356–60. https://doi.org/10.1016/S0043-1648(01)00769-4.
[36] Franco LA, Sinatora A. Material removal factor (fab): a critical assessment of its role in theoretical and practical approaches to abrasive wear of ductile materials. Wear 2017;382–383:51–61. https://doi.org/10.1016/J.WEAR.2017.04.006.
[37] García de Jalón J. Kinematic and dynamic simulation of multibody systems the real-time challenge. 1994.
[38] 3M™ CubitronTM II cut-off wheels | 3M United States. https://www.3m.com/3M/en_US/p/d/b49000239/. Accessed 1 Sep 2021.
[39] Wu C, Li B, Yang J, Liang SY. Prediction of grinding force for brittle materials considering co-existing of ductility and brittleness. Int J Adv Manuf Technol 2016;87:1967–75. https://doi.org/10.1007/s00170-016-8594-4.
[40] Marinescu ID, Rowe B, Ling Y, Wobker HG. Abrasive processes. In: Handbook of ceramics grinding and polishing. Elsevier; 2015. p. 67–132.
[41] Handbook of ceramics grinding and polishing. Handb Ceram Grind Polishing 2015. https://doi.org/10.1016/C2011-0-04219-9.
[42] Kompella S, Zhang K Improved superalloy grinding performance with novel CBN crystals.
[43] Srinivasan B, Rao R, Rao BC, Singh J, Gill S, Dogra M Machinability improvement of inconel 718 during heat treatment-a review you may also like on the development of a dual-layered diamond-coated tool for the effective machining of titanium Ti-6Al-4V alloy A review on cutting fluids used in machining processes. https://doi.org/10.1088/1742-6596/1706/1/012175.
[44] Marinescu ID, Rowe WB, Dimitrov B, Inasaki I. Tribology of abrasive machining processes. 2004.
[45] Baksa T, Hronek O, Farsky J, Zetek M 28TH daaam international symposium ON intelligent manufacturing and automation influence OF cutting conditions ON the surface quality and grinding wheel wear during cylindrical grinding OF inconel 718. 500–0505 . https://doi.org/10.2507/28th.daaam.proceedings.070.
[46] Tso PL. Study on the grinding of Inconel 718. J Mater Process Technol 1995;55:421–6. https://doi.org/10.1016/0924-0136(95)02026-8.
[47] Abachi P, Naseri PSZ, Coyle KP, Tw. Fracture behavior evaluation of high-strength 7050 and 7075 aluminum alloys

using V-notched specimen. Fract mech - prop patterns behav 2016. https://doi.org/10.5772/64463.

[48] Liu H, Zhang J, Xu X, Jiang Y, He Y, Zhao W. Effect of microstructure evolution on chip formation and fracture during high-speed cutting of single phase metals. Int J Adv Manuf Technol 2016;91(1):823–33. https://doi.org/10.1007/S00170-016-9823-6.

[49] Precision abrasive grinding in the 21st century: conventional, ceramic, semi ... - Harry G. Sachsel, C.A.E. - Google Books. https://books.google.es/books?id=3bgJQRkE7lgC&pg=PA496&lpg=PA496&dq=CBN+and+cubitron+are+the+same&source=bl&ots=r562sVtD0M&sig=ACfU3U0nqenWN8iTuHz6uMivITFzfME1FQ&hl=en&sa=X&ved=2ahUKEwiHiO6wg8zyAhUDxoUKHQj1BWsQ6AF6BAgxEAM#v=onepage&q=CBN and cubitron are the same&f=false. Accessed 25 Aug 2021.

[50] Aluminum 1100-O. http://www.matweb.com/search/datasheet_print.aspx?matguid=db0307742df14c8f817bd8d62207368e. Accessed 11 May 2021.

[51] Copper, Cu; annealed. http://www.matweb.com/search/datasheet_print.aspx?matguid=9aebe83845c04c1db5126fada6f76f7e. Accessed 26 Aug 2021.

[52] Advanced machining processes: innovative modeling techniques - Google Books. https://books.google.es/books?id=PhBADwAAQBAJ&pg=PT59&lpg=PT59&dq=fracture+of+Al+1100+during+machining&source=bl&ots=-Fkmwq46VQ&sig=ACfU3U1wqJcbQ_x5ETgktoRQdVaD1CdtNg&hl=en&sa=X&ved=2ahUKEwiPwPb4ss_yAhWGSsAKHQI6BFcQ6AF6BAgkEAM#v=snippet&q=dislocation&f=false. Accessed 26 Aug 2021.

[53] Huang S, Khan AS. Modeling the mechanical behaviour of 1100-0 aluminum at different strain rates by the bodner-partom model. Int J Plast 1992;8:501–17. https://doi.org/10.1016/0749-6419(92)90028-B.

[54] Ni H, Elmadagli M, Alpas AT. Mechanical properties and microstructures of 1100 aluminum subjected to dry machining. Mater Sci Eng, A 2004;385:267–78. https://doi.org/10.1016/J.MSEA.2004.06.048.

[55] Öpöz TT, Chen X. Experimental investigation of material removal mechanism in single grit grinding. Int J Mach Tool Manufact 2012;63:32–40. https://doi.org/10.1016/J.IJMACHTOOLS.2012.07.010.

[56] Patil DV, Ghosh S, Ghosh A, Chattopadhyay AK, Chattopadhyay AB. On grindability of Inconel 718 under high efficiency deep grinding by monolayer cBN wheel. Int J Abras Technol 2007;1:173–86. https://doi.org/10.1504/IJAT.2007.015382.